

AD-A264 266



2

OFFICE OF NAVAL RESEARCH

R&T Project Code 413 a 001

Contract No. N00014-89-J-1235

Technical Report No. 17

1993

Laser-Assisted Chemical Vapor Deposition of InN on Si(100)

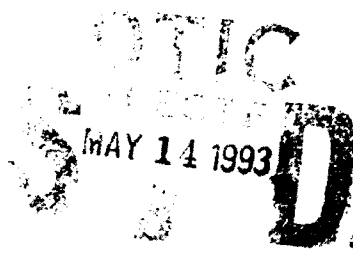
by

Y. Bu, and M. C. Lin

Department of Chemistry

Emory University

Atlanta, GA 30322



Prepared for Publication

in the

Journal Vacuum Science and Technology

Reproduction in whole or in part is permitted for any purpose of the  
United States Government

This document has been approved for public release and sale;  
its distribution is unlimited.

93-10489



93 5 11 15 6

## Abstract

Laser-assisted chemical vapor deposition of InN on Si(100) using  $\text{HN}_3$  and trimethyl indium (TMIn) with and without 308-nm photon excitation has been studied with XPS, UPS and SEM. Without 308-nm excimer laser irradiation, no InN film was built on the surface under the present low-pressure conditions. When the photon beam was introduced, InN films with In:N atomic ratio of  $1.0 \pm 0.1$  and a thickness of more than 20 Å (the limit of the electron escaping depth for the  $\text{In}_{3d}$  X-ray photoelectrons) were formed at temperatures of 300 to 700 K. The He(II) UP spectra taken from these InN films agree well with the result of a pseudo-potential calculation for the InN valence band. Our XPS measurements indicate a 3-D island growth of InN on Si(100) at 700 K, which is confirmed by the SEM images. Although the SEM images taken from the same samples with 2,000 X magnification showed very smooth InN films, InN islands of about 100 nm in diameter could be clearly observed with a magnification of  $\geq 20,000$  X. In contrast, the InN film grown at 300 K showed valleys of uncovered substrate instead of InN islands. These uncovered substrate areas, corresponding to about 5% of the surface exposed to the probing X-ray radiation, probably result from incomplete decomposition of In-C bonds and poor diffusion kinetics at this temperature. Above 800 K, dissociation and desorption of In- and N-containing species occurred and thus no InN film was formed on the surface.

## I. INTRODUCTION

The growth of III-V nitride semiconductors has been a subject of much interest in the past decade. Because of their wide direct band-gaps, these materials have potential uses for electronic and optoelectronic devices such as visible-light

semiconductor lasers, ultraviolet light detectors and laser diodes. However, few publications have appeared in the literature regarding the growth of InN crystals or thin films, probably because InN has a low dissociation temperature and thus low-temperature growth is required.<sup>1,2</sup> This requirement makes it more difficult to grow high quality films.

Recently it has been shown that the chemical vapor deposition (CVD) of InN and InGaN on sapphire substrates can be achieved by using TMIn, TEGa and NH<sub>3</sub> with plasma enhancement under extremely high V/III ratios ( $>10^4$ ).<sup>3</sup> Other methods, such as reactive rf-sputtering and ion plating have also been tried in order to produce the InN films.<sup>7-10</sup> Using low energy In<sup>+</sup> and N<sub>2</sub><sup>+</sup> ion beams, Bello et al.<sup>11</sup> were able to grow InN on a Si(100) surface; however, the resulting InN showed an N:In atomic ratio of  $<0.4$ . The growing of InN films on Si substrates is more difficult probably because of lattice mismatch and silicon nitride formation.

We have recently investigated the photodissociation of HN<sub>3</sub> adsorbed on Si; it was found that atomic N, an effective N species for the nitride film growth, could be generated when an HN<sub>3</sub>-dosed Si sample was exposed to 308-nm laser radiation at a very low surface temperature, i.e., 100 K.<sup>12</sup> In addition, HN<sub>3</sub> has been used for thermal CVD of GaN and Si nitride.<sup>12-15</sup> In the present work, we have utilized the beneficial effect of UV photons to promote InN film deposition. Earlier, Donnelly<sup>16</sup> found that excimer-laser excitation could enhance CH<sub>3</sub> desorption with respect to Ga-containing species, as compared with that observed in the thermal decomposition of TMGa on GaAs surfaces. Consequently, the desorption of the Ga-containing species was suppressed in favor of further decomposition of TMGa to deposit Ga on the surface. Accordingly, the C-contamination was also reduced in the laser-induced decomposition process. The growth of InN films at low substrate temperatures should therefore be achievable by codosing HN<sub>3</sub> and TMIn under the influence of UV

radiation. In this paper, we report the result of the low-pressure CVD of InN on Si(100)-2x1 using TMIn and  $\text{HN}_3$ , aided by 308-nm photon excitation.

## II. EXPERIMENTAL

The present experiment was carried out in a custom-designed (Leybold, Inc.) ultra-high vacuum (UHV) system (Leybold, Inc.) which is composed of two compartments, one for the surface analysis as described elsewhere<sup>15,17</sup> and the other for film deposition. The deposition compartment is further separated into two chambers by a skimmer with a 2-mm diameter hole. The top chamber, equipped with a quadrupole mass spectrometer (QMS) for gaseous product analysis, is differentially pumped by an ST-360 turbo-molecular pump and its base pressure is  $1 \times 10^{-9}$  torr. The second chamber is equipped with an ion sputtering gun for the surface cleaning and is pumped by another ST-360 turbo-molecular pump so that its base pressure is typically at  $5 \times 10^{-9}$  torr.

$\text{HN}_3$  and TMIn samples were prepared in the same manner as described in refs.<sup>15,18</sup> Their vapors over the crystalline TMIn at room temperature (RT) and liquid  $\text{HN}_3$  in a dry ice-alcohol bath were used as the effusive beam sources. They were introduced into the system through two separate 1/8" stainless steel tubes, whose ends were approximately 1/2" above the surface. The gas flow rates were controlled by a combined metering and shut-off valves and monitored by the ion gauge in the deposition chamber.

A Lambda-Physik excimer laser was operated at 308 nm and a repetition rate of 10 Hz with a fluence of 60 mJ/cm<sup>2</sup>.pulse. The photon beam passed through a quartz

window (>95% transmission) and interacted with the surface at an angle of 60° from the surface normal.

An Si(100) single crystal from Virginia Semiconductor Inc. was cut into 0.5 cm x 1.5 cm samples. They were cleaned with hot 5% hydrogen fluoride (HF) solution and then annealed at 1500 K *in vacuo*. The cleanness of the surface was checked with X-ray photoelectron spectroscopy (XPS) and low energy electron diffraction (LEED) before deposition. After a designated deposition time, the sample was moved into the surface analysis chamber for XPS and ultraviolet photoelectron spectroscopy (UPS) measurements and then moved back to the deposition chamber for continuing film deposition. When the deposition was finished, the samples were taken out of the vacuum chamber and stored in N<sub>2</sub> atmosphere before scanning electron microscopy (SEM) measurements.

### III. RESULTS AND DISCUSSION

#### A. XPS Analysis

Fig. 1 shows the dependence of In<sub>3d 5/2</sub> XPS signal intensity on deposition time with and without 308-nm laser irradiation of the substrate. The typical experimental conditions were  $P_{\text{TMIIn}} = 2 \times 10^{-7}$  torr,  $P_{\text{HN}_3} = 1 \times 10^{-6}$  torr, and  $T_s = 700$  K. The excimer laser was operated at a repetition rate of 10 Hz with a fluence of about 60 mJ/cm<sup>2</sup>.pulse. Without laser irradiation, the In XPS signal showed an initial increase and then saturated at a value corresponding to about 1 ML TMIn adsorbed on the surface. No evidence of InN film growth was found within 24 hours, the longest experiment carried out in the present study. When the 308-nm photon beam was introduced, the In XPS signal showed a small initial increase for the first few hours

followed by a rapid change at about 10 hours before it reached a saturation value. The observed saturation of the In signal is likely limited by the electron escaping depth rather than by the ending of the InN film growth, since the corresponding Si<sub>2p</sub> XPS signal dropped to zero after 10 hours of InN deposition.

The disappearance of the Si XPS signal also allows us to determine that the InN film thickness is  $\geq 20$  Å. In addition, the intensity ratio of In:N reached a value of  $\sim 0.9$  above the saturation point, if the photo-emission cross-sections for N<sub>1s</sub> and In<sub>3d 5/2</sub> were taken into account.<sup>19</sup> This observation indicates a stoichiometric or nearly stoichiometric growth of InN film under the indicated experimental conditions. Further growth of the InN film could not be characterized by the XPS technique.

The observed growth behavior of the In XPS signal showed a typical Volmer-Weber mechanism, i.e., a 3-D island growth mode.<sup>20</sup> Indeed, islands with a diameter of about 100 nm were clearly observed in SEM images taken from the InN films grown at different times and the number of the islands increased as the deposition time was increased. The island growth of InN on Si(100) is expected, because Si(100)-2x1 surface and InN crystals have very different lattice structures and chemical properties. Recently, Snyder et al.<sup>21</sup> have shown that the lattice mismatch value  $>2-3\%$  could lead to 3-D island nucleation, even though material structures and chemical properties are similar; e.g., the growth of InGaAs on GaAs(100).

Shown in Fig. 2 are a few XPS spectra taken from a clean Si surface and from the InN films grown on the Si surface at different deposition times denoted by b, c and d in Fig. 1. The clean Si(100) spectrum presented two major peaks at 153 and 101.5 eV due to Si<sub>2s</sub> and Si<sub>2p</sub> photoelectrons, respectively. Other features attributable to the Si<sub>2p</sub> shake-up at 170, 118 and Si<sub>MNN</sub> Auger electrons at 425, 475 eV, respectively, also appeared in the spectrum. In addition, a weak signal originated from Ta<sub>4d</sub>

photoelectrons (Ta clips were used to hold Si substrate in the present study) at ~230 eV was noted in the spectrum. When the film deposition time was increased, the signals from the clean sample decreased while those of  $\text{In}_{3d\ 3/2}$ ,  $\text{In}_{3d\ 5/2}$  and  $\text{N}_{1s}$  at 452, 444.4 and 396.6 eV, respectively, increased. A peak at 435 eV due to  $\text{In}_{3d\ 5/2}$  photoelectrons excited by Mg  $\text{K}\alpha_3$  and  $\text{K}\alpha_4$  photons also appeared in spectra b, c and d. Furthermore, the atomic ratio of In:N increased with increasing deposition time, because the  $\text{N}_{1s}$  signal from other N-containing species,  $\text{SiNH}_x$ , was suppressed. In spectra c and d, the Si XPS signals were within the noise level. Interestingly and importantly, the near-absence of any  $\text{C}_{1s}$  XPS signal in all spectra suggests that C contamination in the deposited InN film under the experimental conditions is not as serious as that implied by the TMIn thermal decomposition results.<sup>18</sup> It was found that after the dissociation of the In-C bonds in TMIn on Si substrates, partial  $\text{CH}_x$  species remained on the surface at temperatures higher than the In desorption temperature. Similar observations were reported for TMAI and TMGa on Si surfaces.<sup>22,23</sup> Clearly, the reaction mechanisms are different in the thermal decomposition of TMIn on Si than in the InN film deposition process using TMIn,  $\text{HN}_3$  and 308-nm photon beams. In the latter case, the formation of the InN bond may facilitate the release of  $\text{CH}_3$  radicals. The photon also stimulates the breaking of the In-C bonds and the desorption of C-containing species<sup>16</sup> during the InN film deposition process.

The  $\text{In}_{3d\ 5/2}$ ,  $\text{Si}_{2p}$  and  $\text{N}_{1s}$  XPS signals were further examined by scanning the spectra over smaller energy ranges as shown in Fig. 3a, b and c, respectively. The In XPS spectra give a single peak at 444.4 eV with an FWHM of 1.8 eV for all three cases. Such a peak was observed earlier for an  $\text{InN}_{0.4}$  film on Si(100) prepared by using low energy  $\text{In}^+$  and  $\text{N}_2^+$  ion beams.<sup>11</sup> The peak is higher in binding energy than that of the elemental In (443.7 eV) as reported by Bello et al.<sup>11</sup> and by Bu et al.<sup>18</sup> for TMIn on Si surfaces after the complete dissociation of the In-C bonds and the

formation of In islands on the substrates at 600-700 K. On the other hand, both  $N_{1s}$  and  $Si_{2p}$  signals showed more than one N and Si components in their XPS spectra, indicating that  $SiN_x$  and probably some  $NH_x$  species were also formed in the InN film deposition process. Two peaks at 99.5 and 101.5 eV were noted in the  $Si_{2p}$  XPS spectra in Fig. 3b; they could be attributed to the clean Si and Si in Si nitride, respectively.<sup>24</sup> As the deposition time increased, both peak intensities decreased and then disappeared totally because of the suppression by the InN film.

The corresponding  $N_{1s}$  XPS spectra are shown in Fig. 3c. The bottom curve revealed a broad  $N_{1s}$  band at 397.9 eV with an FWHM of ~2.3 eV, which could be deconvoluted into two peaks at 397.9 and 396.6 eV. The latter peak is due to  $N_{1s}$  in InN<sup>11</sup> and the 397.9 peak is attributable to  $N_{1s}$  in Si nitride, which indicates the formation of Si nitride during the film deposition process as also clearly indicated by the  $Si_{2p}$  XPS peak at 101.5 eV. The  $N_{1s}$  XPS peak in Si nitride was reported at 397.4 and 397.7 eV.<sup>25,26</sup> The observed peak centered at 397.9 eV because of the partial contribution from the  $NH_x$  species, which showed peaks at 388.5 and 388.8 eV for NH and  $NH_2$  species on Si(100), respectively.<sup>25,26</sup> As the deposition time increased, the 396.6 eV peak became the dominant feature in  $N_{1s}$  XPS spectrum because of the growth of InN on the surface. In contrast, the 397.9 eV peak was reduced and shifted to 398.3 eV. Recalling the gradual disappearance of the  $Si_{2p}$  XPS signals under the same experimental conditions, shown in Fig. 2, the changes of the 397.9 eV peak suggest that the 398.3 eV component in  $N_{1s}$  XPS spectrum is not due to Si nitride. We attribute this peak to the  $NH_x$  species, likely on the surface of the InN film or islands, which tend to terminate the film growth until further laser irradiation is applied to break the NH bond. The presence of  $NH_x$  species is not surprising, because it is the primary product in the photolysis of the gaseous  $HN_3$  and one of the key products in the photodissociation of  $HN_3$  adsorbed on Si substrates.<sup>12</sup> Employing a higher



energy photon beam to operate the laser at a higher fluence and higher repetition rate may dissociate NH bonds more efficiently and hence reduce the  $\text{NH}_x$  species. The formation of the  $\text{SiN}_x$  species in the early stages of film deposition, on the other hand, is probably inevitable. The SiN bond strength is strong and the  $\text{SiN}_x$  species was formed during the surface photolysis of  $\text{HN}_3$  on Si.<sup>12</sup> The  $\text{SiN}_x$  was also found in the InN film deposition process using  $\text{In}^+$  and  $\text{N}_2^+$  ion beams,<sup>11</sup> where an atomic ratio of less than 0.4 was reported for N:In as alluded to above. In the present study, we found that the In:N ratio is  $\sim 0.9$ , which becomes 1.1 if the 398.3 eV component is excluded. The In:N ratio of our deposited film therefore averaged about  $1.0 \pm 0.1$ .

Fig. 4 illustrates the effect of substrate temperature on InN film growth on Si(100). At room temperature, thick layers ( $\geq 20 \text{ \AA}$ ) of InN were also developed. However, C contamination was obvious (see Fig. 4a), probably because of the incomplete In-C bond breaking and poor diffusion kinetics at lower surface temperatures. Nevertheless, the growth of InN film at RT with the help of photon excitation is achievable and the film seemed to be smoother than that grown at 700 K (see SEM results). Carbon contamination could be reduced by using other In sources, such as In,  $\text{InX}_3$ , and  $\text{TEIn}$ . It could also be reduced by increasing the deposition temperature. As shown in Fig. 4b, essentially no  $\text{C}_{1s}$  XPS signal appeared in the 700 K spectrum (Fig. 4b), because of the complete dissociation of the In-C bonds and the desorption of C-containing species. However, as the surface temperature was further increased to 800 K, no InN film was obtained under otherwise the same dosing conditions (Fig. 4c). In this case, the  $\text{Si}_{2p}$  XPS signal was attenuated slightly and the  $\text{In}_{3d_{5/2}}$  XPS signal was only about 6% of that obtained at 700 K. Above 873 K, In droplets instead of InN were observed on  $\text{Al}_2\text{O}_3$  surfaces.<sup>5</sup> This temperature dependence agrees reasonably well with the result observed here, especially

considering the different substrates used and the effect of laser excitation in the present study.

## B. UPS Analysis

The InN films made in the present study were also characterized with the UPS technique; a representative spectrum is shown in Fig. 5. The measured He(II) UPS spectrum is compared with a theoretical spectrum calculated by a pseudo-potential method.<sup>27</sup> The experimental spectrum was aligned with the calculated curve at zero energy. Good agreement between the two results was obtained. Both curves showed a maximum at 2.1 eV and two other peaks at higher energies. However, the doublet at 6.5 and 7.1 eV was not resolved in our UPS spectrum. Instead, a broad band at 6.6 eV is observed and a shoulder at 8.5 eV was more pronounced; accordingly, the overall valence band width was greater than the theoretical value. The intense peak at ~16.7 eV, which is not presented in the theoretical curve, is due to the In<sub>4d</sub> photoelectrons. The In<sub>4d</sub> 3/2 and In<sub>4d</sub> 5/2 peaks were separated when TMIn was dosed on Si substrates,<sup>18</sup> but here the two peaks overlapped to give one band at 16.7 eV. In our unpublished work, an identical UPS spectrum was obtained for InN on GaAs(110) suggesting that the substrate contribution to the spectra is negligible as expected (due to the suppressing effect of the thick InN layers).

## C. SEM Analysis

The morphologies of several InN films grown on Si(100) under various conditions are examined with SEM as shown in Figs. 6 and 7. When grown at 700 K, the InN film seemed to be very smooth as indicated by the SEM image with a magnification of 2000 times (Fig. 6a), a typical magnification used in the literature for InN and GaN films deposited by other methods.<sup>3,5</sup> Annealing the sample at 850 K caused no obvious change in SEM image at this scale (Fig. 6b). On the other hand,

the SEM image from the InN film grown at RT revealed some uncovered areas of the substrate (see Fig. 6c). In consistence with the SEM results, our XPS measurement showed an Si<sub>2p</sub> signal corresponding to 5% of that taken from the clean surface, which suggests that the uncovered surface area is about 5% of the total surface exposed to X-ray radiation. Fig. 6d shows an SEM image taken from a partially developed InN sample, which gave an In<sub>3d 5/2</sub> signal intensity equal to 25% that of the saturation value; this corresponds to the deposition time at point b in Fig. 1. In this case, some dark areas due to the Si substrate are evident, confirming the 3-D island nucleation result established from XPS analyses. Such an island growth of InN on Si(100) could be viewed unambiguously from the SEM images taken from the same samples at a magnification factor of 20,000 (see Fig. 7). It can be seen from Fig. 7a that InN islands with a diameter of about 100 nm were rather evenly distributed on the surface. When the sample prepared under the same conditions was annealed at 850 K for a few minutes, the diameter of the InN islands was reduced by a few times, as shown in Fig. 7b. The In<sub>3d 5/2</sub> XPS signal intensity from this post-annealed sample was also reduced by 20% from its saturation value, i.e., the value obtained before annealing the sample. Meanwhile, the Si<sub>2p</sub> XPS signal corresponding to 10% of that of the clean Si was recovered. These changes are obviously due to the partial decomposition of InN and the desorption of some N and In containing species. The desorption of N-containing species is apparently more significant as indicated by the increase of the In:N atomic ratio from 0.9 to 1.5 upon the annealing of the sample at 850 K. This observation is consistent with the reported low InN dissociating temperature and the high equilibrium nitrogen pressure over the solid InN.

Finally, the InN film grown at RT is different from those grown at 700 K. Instead of InN islands, valleys were observed in SEM images as shown in Fig. 7c. This is

likely because, at lower substrate temperatures, the 3-D island nucleation may be limited by poor surface-diffusion kinetics.<sup>21</sup>

## **VI. CONCLUSION**

Using  $\text{HN}_3$ ,  $\text{TlIn}$  and 308-nm photon beams,  $\text{InN}$  films could be formed on  $\text{Si}(100)$  at 300 and 700 K under low-pressure conditions. Based on the results of XPS analyses, these films have an  $\text{In:N}$  atomic ratio of 0.9 and a thickness of  $>20\text{\AA}$ , the limit of photoelectron escaping depth.  $\text{He(II)}$  UP spectra taken from the deposited  $\text{InN}$  films are in good agreement with that of a pseudo-potential model calculation for  $\text{InN}$ . The corresponding SEM analyses showed smooth  $\text{InN}$  films with a magnification of 2000X. The result obtained from a higher magnification, however, revealed the presence of  $\text{InN}$  islands with diameters of about 100 nm. This observation confirms the 3-D island growth model for  $\text{InN}$  on  $\text{Si}(100)$  at 700 K as established from the XPS measurements. In contrast, valleys corresponding to 5% uncovered substrate surface were observed for the film deposited at 300 K. Above 800 K, the dissociation of  $\text{InN}$  and the desorption of the  $\text{In}$  and  $\text{N}$  containing species occurred and no  $\text{InN}$  film was formed on  $\text{Si}(100)$ .

Under similar low-pressure deposition, no film growth was observed without the assistance of the 308-nm UV radiation.

## **ACKNOWLEDGMENT**

The authors gratefully acknowledge the support of this work by the Office of Naval Research.

## REFERENCES

1. J.B. MacChesney, P.M. Bridenbaugh and P.B. O'Connor; *Mater. Res. Bull.*, 5 (1970) 783.
2. A. Wakahara, T. Tsuchiva and A. Yoshida; *Vacuum* 41 (1990) 1071.
3. T. Matsuoka, H. Tanaka, T. Sasaki and A. Katsui; *Inst. Phys. Conf. Ser. No. 106*: Chapter 3, 141.
4. L.A. Marasina, I.G. Pichugin and M. Tlaczala; *Krist. Tech.*, 12 (1977) 541.
5. A. Wakahara and A. Yoshida; *Appl. Phys. Lett.*, 54 (1989) 709.
6. A. Wakahara, T. Tsuchiya and A. Yoshida; *J. Crystal Growth*, 99 (1990) 385.
7. T.L. Tansley and C.P. Foley; *J. Appl. Phys.* 59 (1986) 3241.
8. B.R. Natarajan, A.H. Eltonkhy, J.E. Green and T.L. Barr; *Thin Solid Films* 69 (1980) 201.
9. H.J. Hovel and J.J. Cuomo; *Appl. Phys. Lett.* 20 (1972) 71.
10. J.W. Trainor and K. Rose; *J. Electron. Mater.* 3 (1974) 821.
11. I. Bello, W.M. Lau, R.P.W. Lawson and K.K. Foo; *J. Vac. Sci. Technol. A*10 (1992) 1642.
12. Y. Bu and M.C. Lin; to be published.
13. M.C. Flowers, N.B.H. Jonathan, A.A.B. Laurie, A. Morris and G.J. Parker; *J. Mater. Chem.* 2 (1992) 365.
14. R. Ishihara, H. Kanoh, O. Sugiura and M. Matsumura; *Jpn. J. Appl. Phys.* 31 (1992) L74.
15. J.C.S. Chu, Y. Bu and M.C. Lin; *Surf. Sci.* 284 (1993) 281.
16. V.M. Donnelly; *J. Vac. Sci. Technol. A*9 (1991) 2887.
17. Y. Bu, D.W. Shinn and M.C. Lin; *Surf. Sci.* 276 (1992) 184.
18. Y. Bu, J.C.S. Chu and M.C. Lin; *Mater. Lett.* 14 (1992) 207.
19. H. Berthou and C.K. Jorgensen; *Analytical Chem.* 47 (1975) 482.

20. J.M. Slaughter, W. Weber, G. Guntherodt and C.M. Falco; Mater. Res. Soc. Bull., Dec. (1992) 39.
21. C.W. Snyder, B.G. Orr, D. Kessler and L.M. Sander; Phys. Rev. Lett. 66 (1991) 3032.
22. T.R. Gow, R. Lin, L.A. Cadwell, F. Lee, A.L. Backman and R.I. Masel; Chem. Mater. 1(1989) 406.
23. F. Lee, A.L. Backman, R. Lin, T.R. Gow and R.I. Masel; Surf. Sci. 216 (1989) 173.
24. R.N.S. Sodhi, W.M. Lau and S.I.J. Ingreys; J. Vac. Sci. Technol. A7 (1989) 663.
25. J.L. Bischoff, F. Lutz, D. Bolmont and L. Kubler; Surf. Sci. 251 (1991) 170.
26. F. Bozso and Ph. Avouris; Phys. Rev. B38 (1988) 3937.
27. C.P. Foley and T.L. Tansley; Phys. Rev. B 33 (1986) 1430.

## Figure Captions:

- Fig. 1 The dependence of  $\text{In}_{3d\ 5/2}$  XPS signals on the InN film deposition time. (O) without 308-nm laser irradiation; ( $\Delta$  and X) for different experimental runs with laser irradiation. The experiments were carried out at  $P_{\text{TMin}} = 2 \times 10^{-7}$  torr,  $P_{\text{HN}_3} = 1 \times 10^{-6}$  torr and  $T_s = 700$  K. Insert details the initial rise of the In signals for the first few hours of deposition with laser irradiation.
- Fig. 2 XPS spectra taken from InN on Si(100) at different deposition times corresponding to b, c and d in Fig. 1. The bottom curve is taken from a clean Si(100) surface.
- Fig. 3  $\text{In}_{3d\ 5/2}$  (3a),  $\text{Si}_{2p}$  (3b) and  $\text{N}_{1s}$  (3c) XPS spectra taken from the same samples as those in Fig. 2 with smaller energy scans.
- Fig. 4. XPS spectra taken from InN grown on Si(100) at 300, 700 and 800 K, respectively. No InN film was formed at 800 K.
- Fig. 5. He(II) UPS spectrum taken from InN grown on Si(100) at 700 K. The dashed line is a pseudo-potential calculation for InN valence band by Foley and Tansley in ref. 27.
- Fig. 6. SEM images taken with a magnification of 2000 X from InN on Si(100): (a) grown at 700 K, (b) annealing at 850 K after grown at 700 K, (c) grown at 300 K and (d) grown at 700 K with a shorter deposition time corresponding to point b in Fig. 1.
- Fig. 7. SEM images taken from the same samples as those in Fig. 6, but with a magnification of 20,000 X.

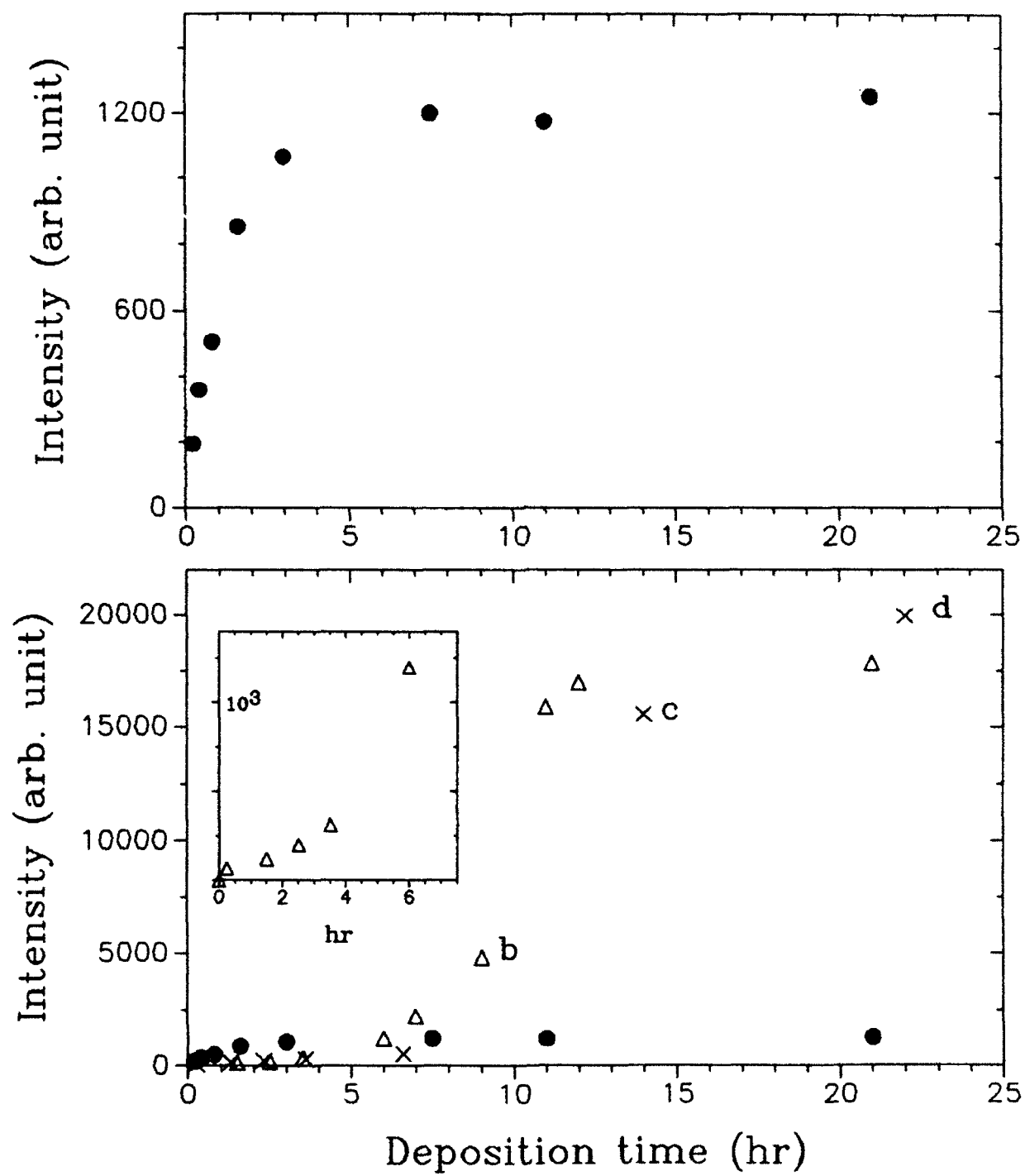




Fig. 2

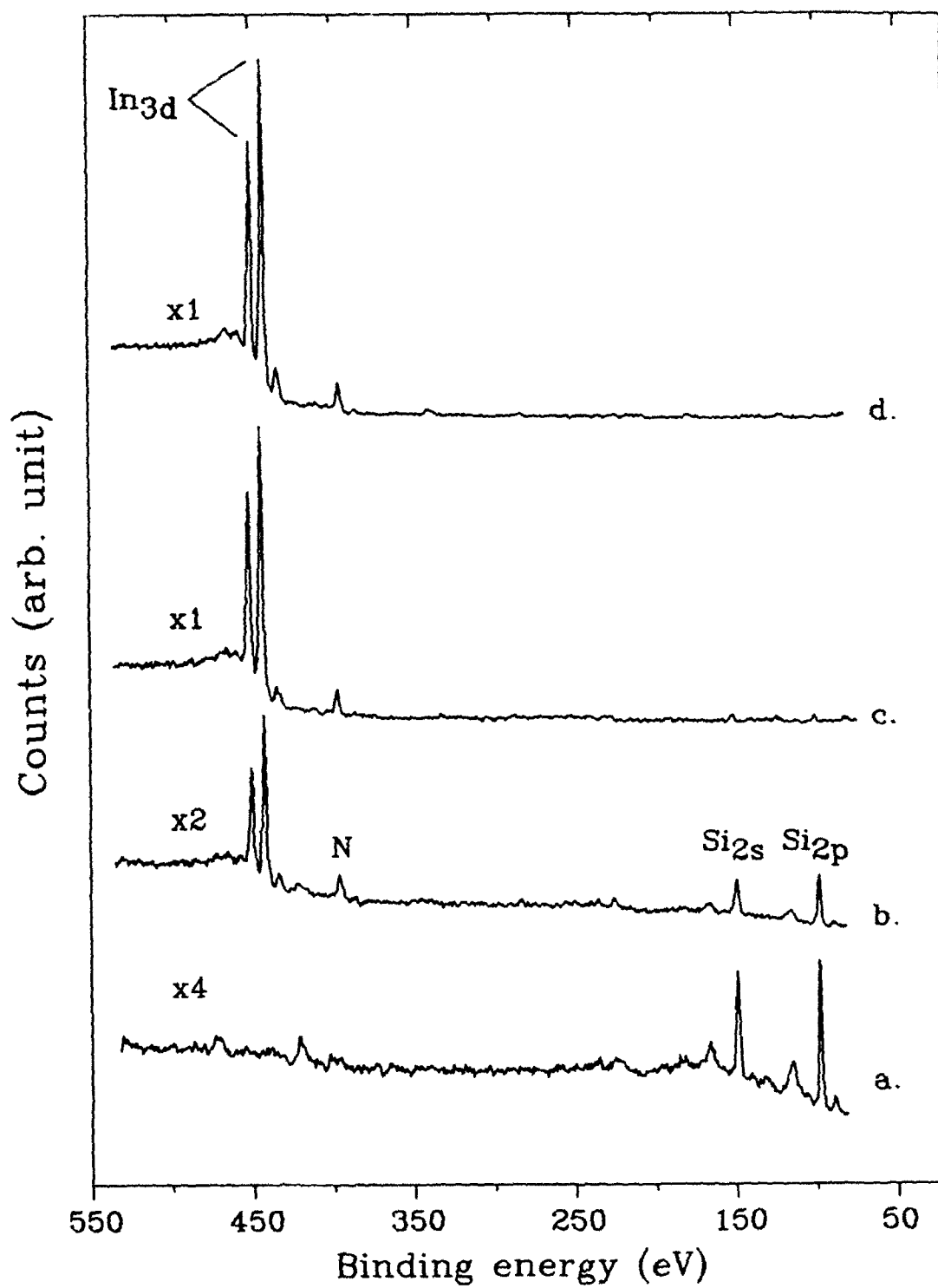


Fig. 3a

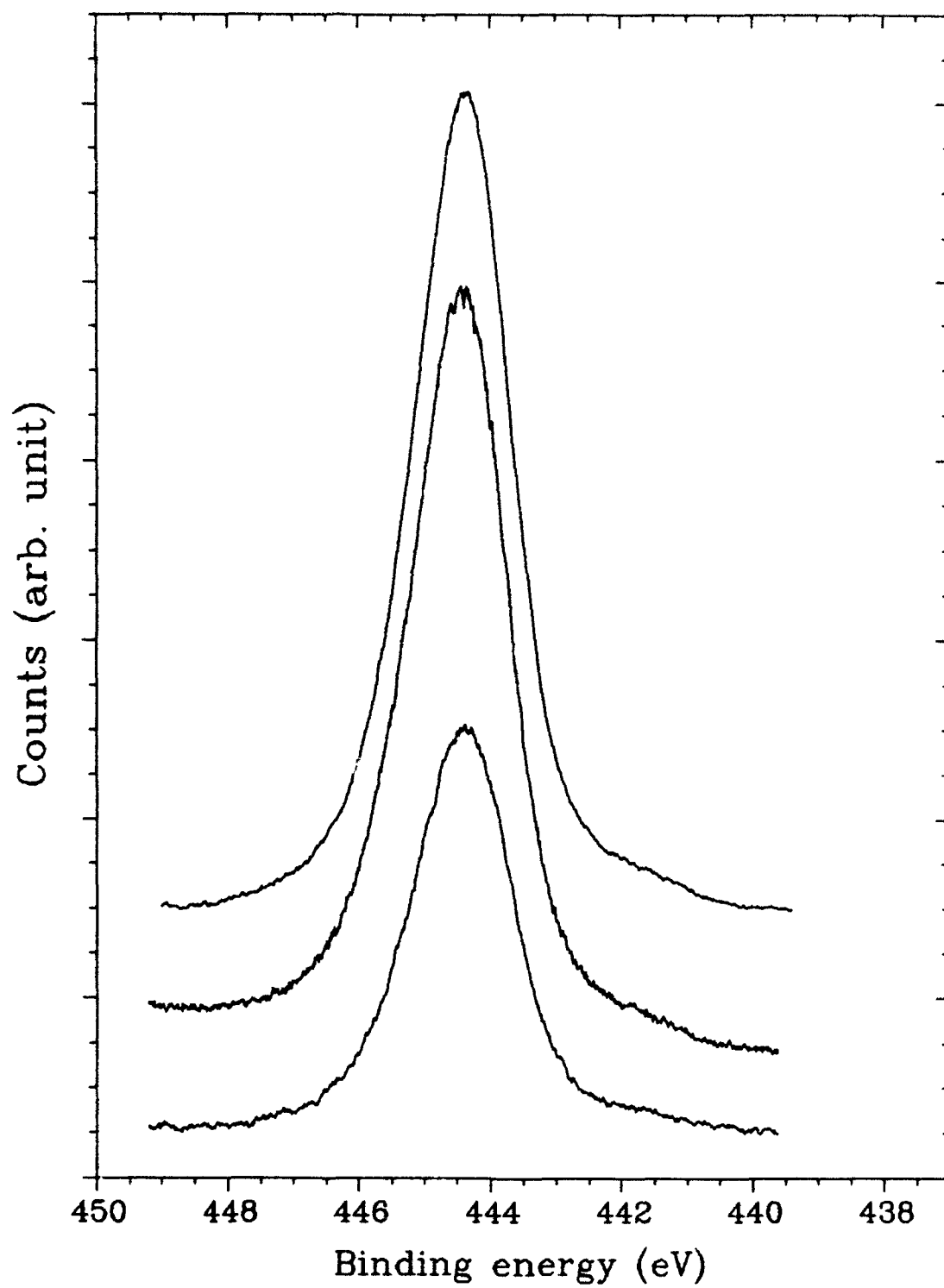


Fig. 3b

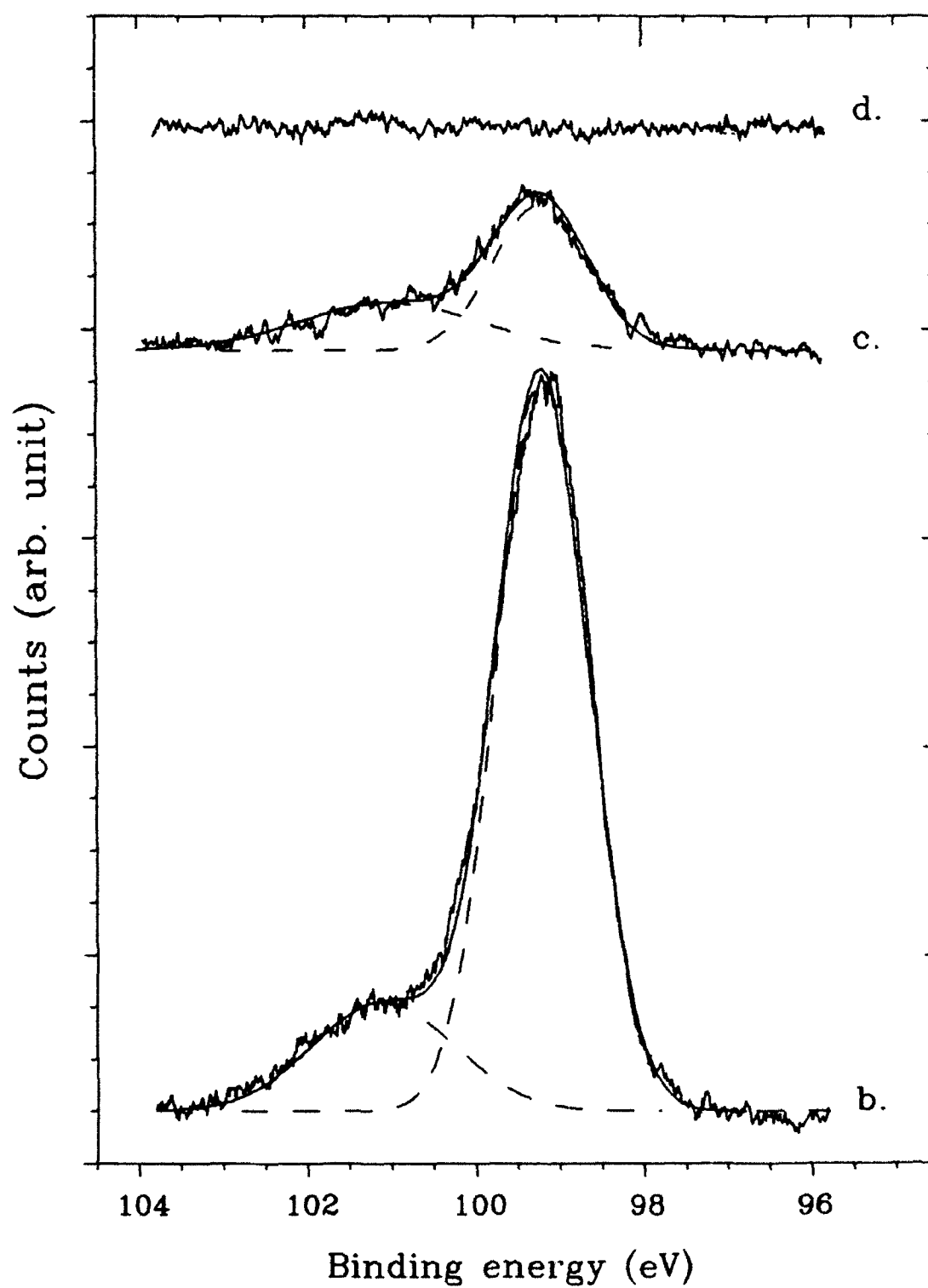
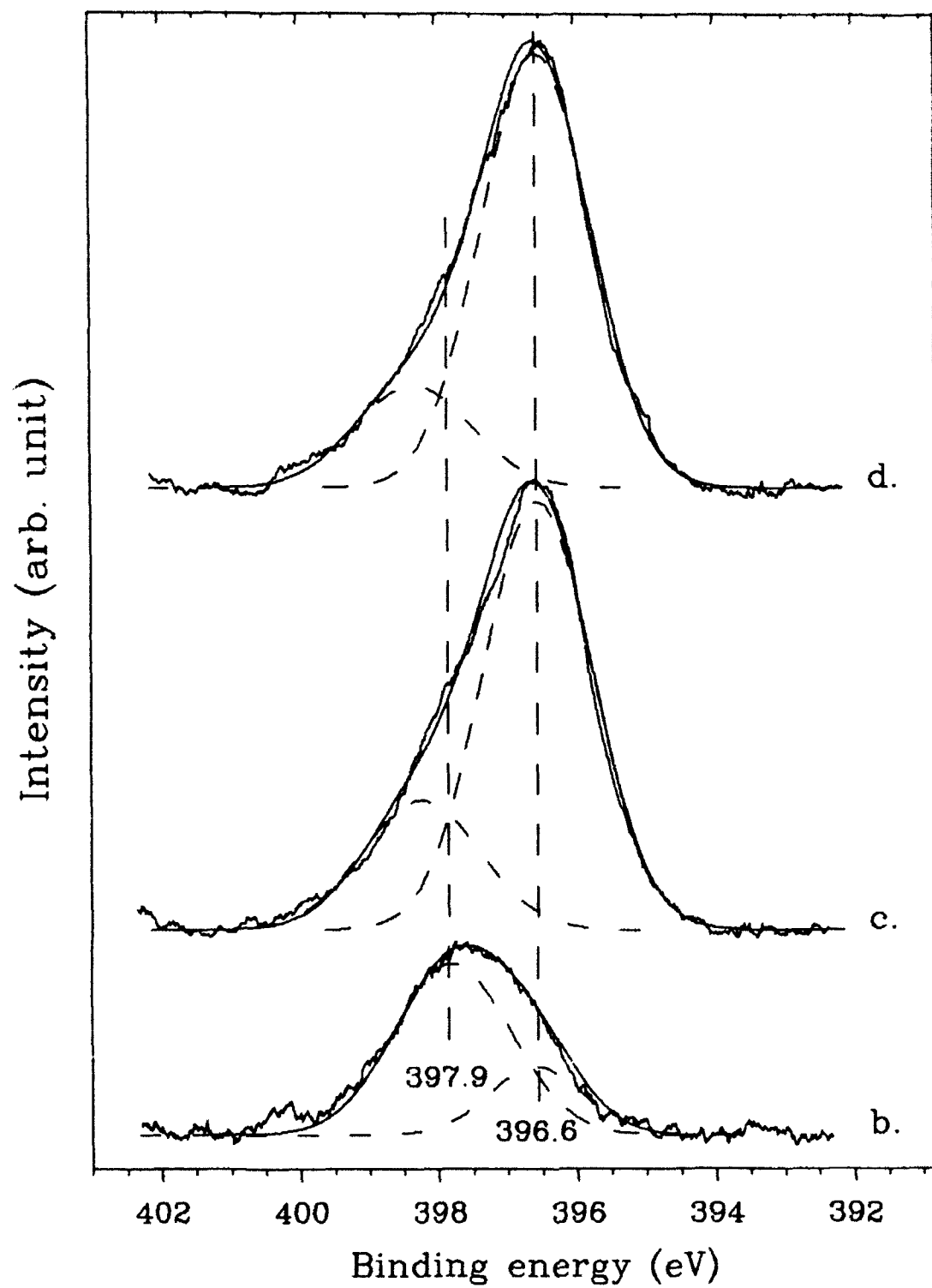


Fig. 3c



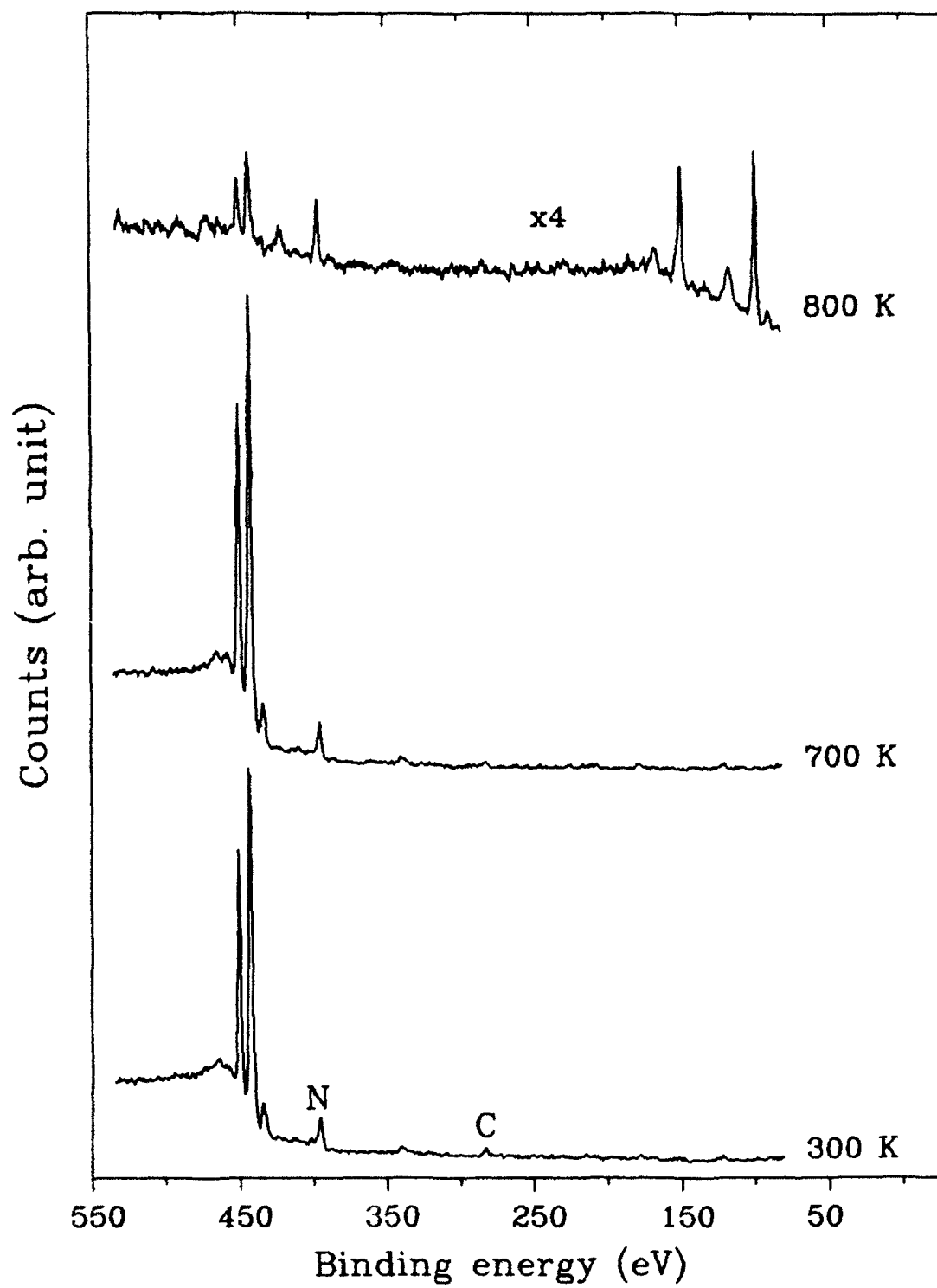
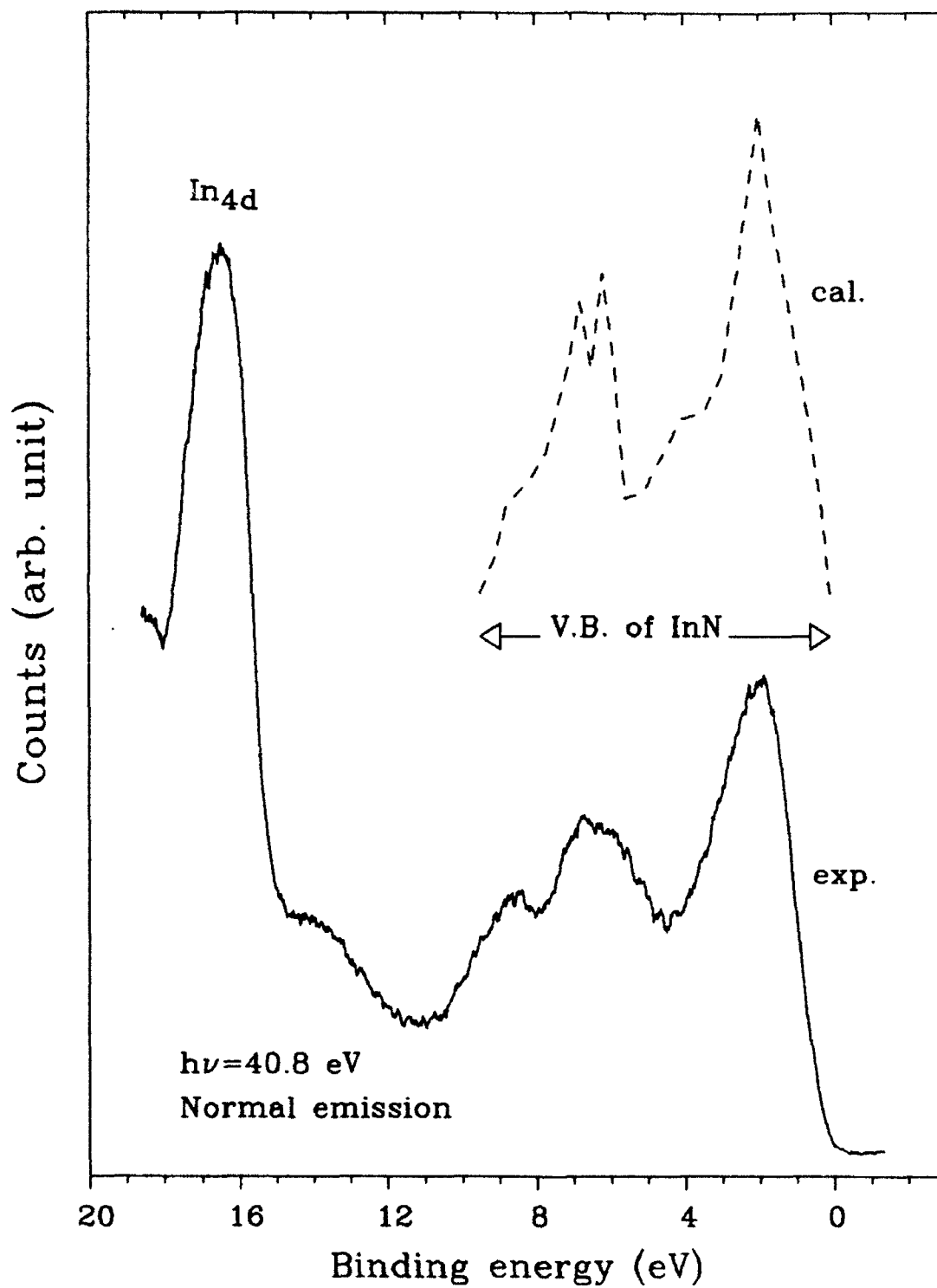


Fig. 5



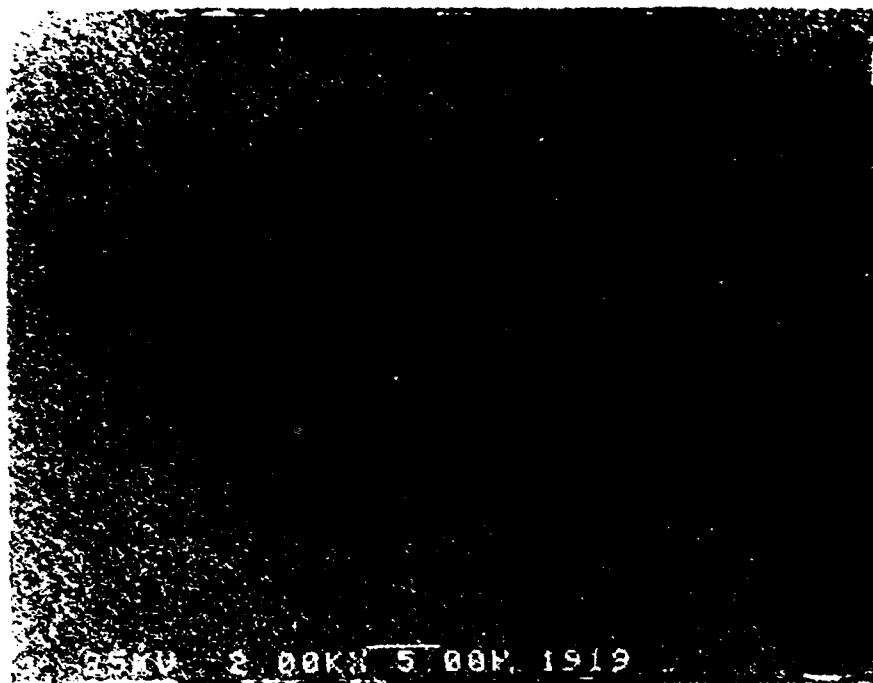


Fig. 6a



Fig. 7a

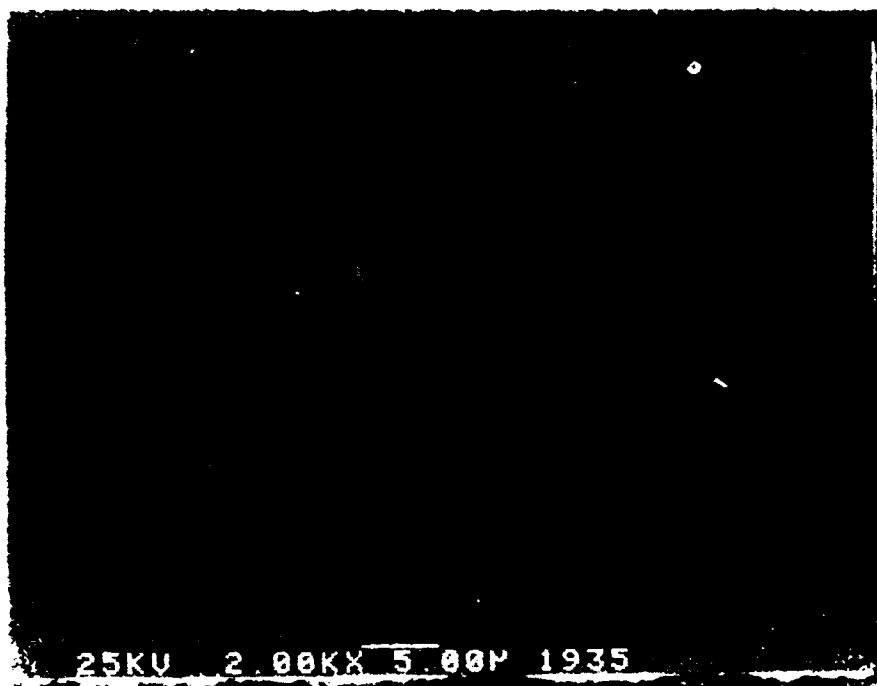


Fig. 6b

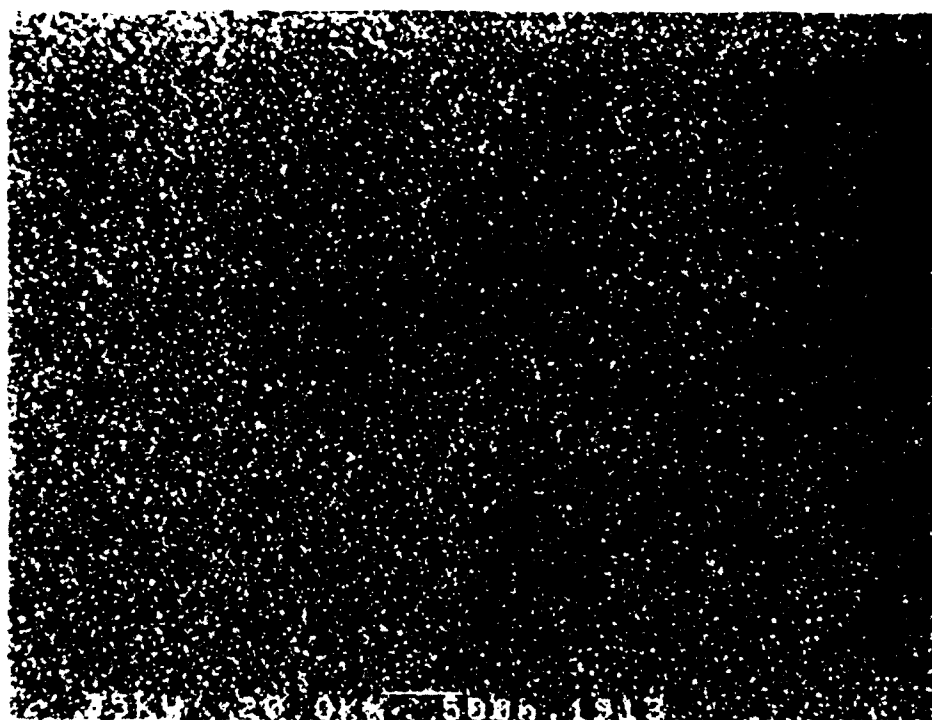


Fig. 7b



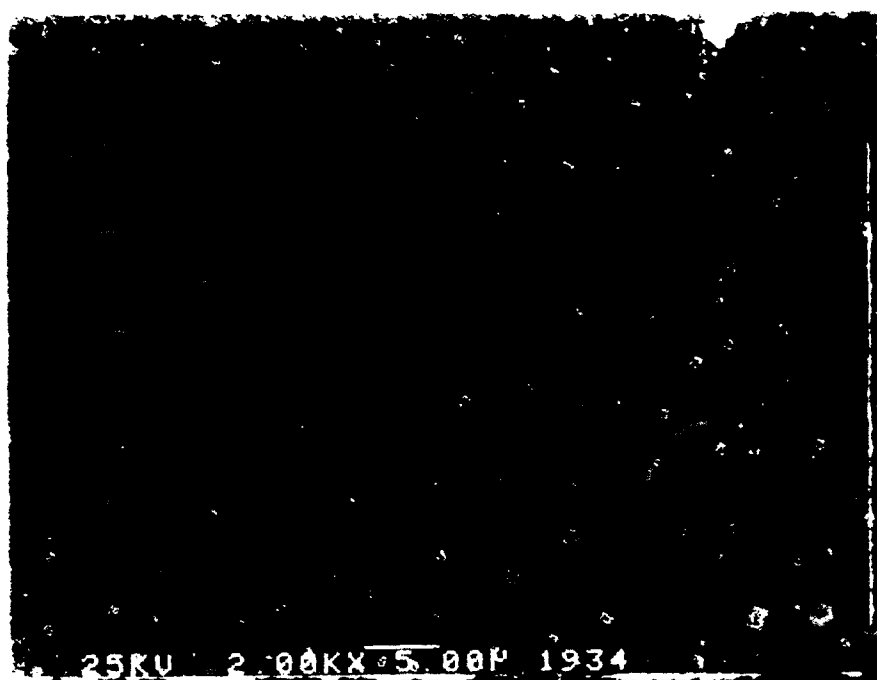


Fig. 6c

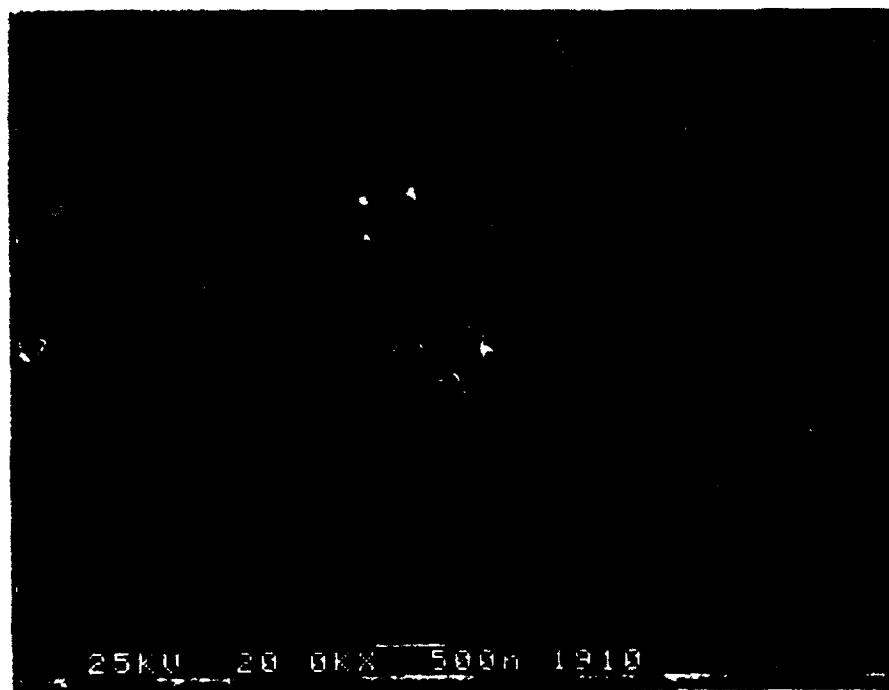


Fig. 7c

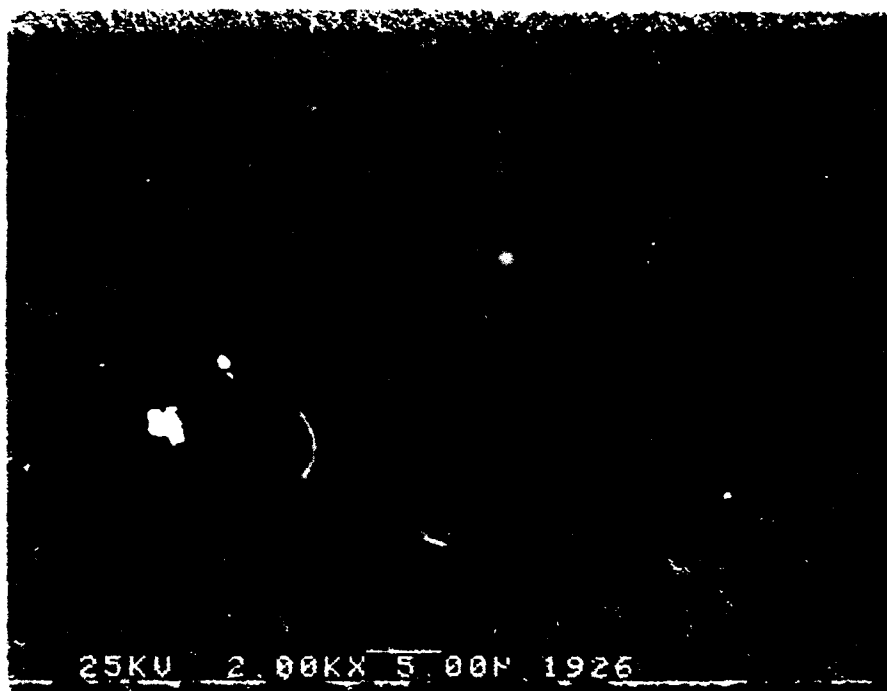


Fig. 6d

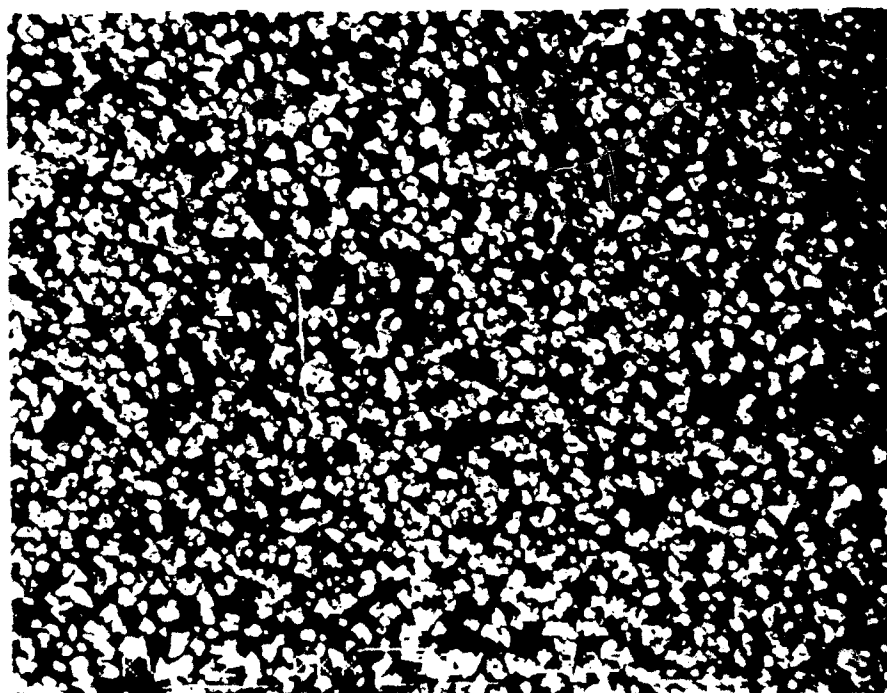


Fig. 7d